



HAL
open science

The geometric phase of bivariate signals

Nicolas Le Bihan, Julien Flamant, Pierre-Olivier Amblard

► **To cite this version:**

Nicolas Le Bihan, Julien Flamant, Pierre-Olivier Amblard. The geometric phase of bivariate signals. 32nd European Signal Processing Conference, EUSIPCO 2024, Aug 2024, Lyon, France. hal-04691994

HAL Id: hal-04691994

<https://hal.science/hal-04691994v1>

Submitted on 9 Sep 2024

HAL is a multi-disciplinary open access archive for the deposit and dissemination of scientific research documents, whether they are published or not. The documents may come from teaching and research institutions in France or abroad, or from public or private research centers.

L'archive ouverte pluridisciplinaire **HAL**, est destinée au dépôt et à la diffusion de documents scientifiques de niveau recherche, publiés ou non, émanant des établissements d'enseignement et de recherche français ou étrangers, des laboratoires publics ou privés.



Distributed under a Creative Commons Attribution 4.0 International License

The geometric phase of bivariate signals

Nicolas Le Bihan
Université Grenoble Alpes,
CNRS, Grenoble INP, GIPSA-lab
Grenoble, France
nicolas.le-bihan@cnrs.fr

Julien Flamant
Université de Lorraine, CNRS, CRAN
Nancy, France
julien.flamant@cnrs.fr

Pierre-Olivier Amblard
Université Grenoble Alpes,
CNRS, Grenoble INP, GIPSA-lab
Grenoble, France
pierre-olivier.amblard@cnrs.fr

Abstract—This paper provides an introduction to an intriguing geometric phenomenon that can occur when considering narrow-band bivariate signals. This so-called geometric phase may appear when the signal normalized second order instantaneous moment follows a smooth curve in the curved projective space. The resulting geometric phase is independent of the signal frequency and magnitude. Well known in quantum mechanics, optics or non-holonomic dynamical systems, the geometric phase can be computed using the concept of Bargmann invariant. It is associated to the time evolution of polarization parameters for bivariate signals. Numerical simulations on signal processing examples illustrate the peculiar phenomenon of geometric phase.

Index Terms—Bivariate signals, time-varying parameters, geometric phase, Bargmann invariant, ray space

I. INTRODUCTION

We consider narrowband AM-FM signals, which for the univariate case can be modeled using the well-known analytic signal [1]. This complex-valued signal gives access to the instantaneous attributes (amplitude and phase) of the original univariate signal. In the bivariate case, four attributes are necessary to fully describe the signal. They can be defined using for example the modulated ellipse model or the analytic signal pairs [2] and their associated attributes/parameters. Alternatively, for the bivariate case, the quaternion embedding [3] is a *geometric* extension of the analytic signal directly parametrized with physics inspired quantities. The different representations available for the bivariate extension of the analytic signal are equivalent, and only differ by their parametrization. Thus, in the sequel, we will use the formalism introduced in [3] in order to make connections with concepts well established in physics (optics and quantum mechanics). First, we briefly review the instantaneous attributes that will be of interest in the sequel and then move to the second order representation for bivariate signals. Section IV then introduces the concept of geometric phase for bivariate signals, and finally a practical way of estimating this phase is proposed, together with illustrative examples.

II. INSTANTANEOUS ATTRIBUTES FOR BIVARIATE SIGNALS

In this section we review known results in the representation and analysis of AM-FM signals, see e.g. [2]–[4] for details. In

Research supported by the ANR project RICOCHET ANR-21-CE48-0013. This project has received financial support from the CNRS through the MITI interdisciplinary programs.

the paper, $L^2(\mathbb{E})$ stands for the vector space of finite energy signals indexed by \mathbb{R} (typically time) with values in \mathbb{E} .

A. Univariate case

A real valued AM-FM signal $s(t) \in L^2(\mathbb{R})$ can be modeled as $s(t) = a(t) \cos \varphi(t)$, where the *instantaneous* amplitude $a(t)$ and phase $\varphi(t)$ (also named the *canonical pair*) are some regular functions of time. It is well known that these two parameters can be unambiguously determined via the complex valued analytic signal $x(t) = s(t) + \mathbf{j} \text{HT} \{s(t)\} \in L^2(\mathbb{C})$ where $\text{HT} \{\cdot\}$ stands for the Hilbert transform and $\mathbf{j}^2 = -1$. Indeed, the polar expression of $x(t) = a(t) \exp(\mathbf{j}\varphi(t))$ is directly driven by the instantaneous parameters that give access to the time evolution of magnitude and phase (assuming Bedrosian's theorem applies [1], [4]). The AM-FM property of $s(t)$ is thus encoded in the variations of $a(t)$ and $\varphi(t)$.

B. Bivariate case

For a real-valued bivariate AM-FM signal $\mathbf{s}(t) = (s_1(t), s_2(t))^T \in L^2(\mathbb{R}^2)$, it is also possible to define a complex-valued *analytic* bivariate signal, denoted $\mathbf{x}(t) \in L^2(\mathbb{C}^2)$. Several definitions of $\mathbf{x}(t)$ have been proposed: modulated ellipse [2], rotary components [5], or quaternion embedding [3]. Despite involving different parameterizations, they all agree that four *instantaneous* parameters are needed to describe the time evolution of $\mathbf{x}(t)$ (or equivalently $\mathbf{s}(t)$), thus giving rise to a *canonical quadruplet* that encodes the signal fluctuations. Using the parametrization introduced in [3], the complex bivariate narrow-band AM-FM signal $\mathbf{x}(t)$ takes the following form:

$$\mathbf{x}(t) = a(t) e^{\mathbf{j}\varphi(t)} \begin{pmatrix} \cos \theta(t) \cos \chi(t) + \mathbf{j} \sin \theta(t) \sin \chi(t) \\ \sin \theta(t) \cos \chi(t) - \mathbf{j} \cos \theta(t) \sin \chi(t) \end{pmatrix} \quad (1)$$

where the canonical quadruplet $[a(t); \theta(t); \chi(t); \varphi(t)]$ completely describes the time evolution of the signal $\mathbf{x}(t)$. Just like the univariate case, some conditions on the dynamics of those parameters apply in order for the geometric interpretation (to be detailed in section III) to be valid. This is the extension of the Bedrosian theorem to the bivariate case, detailed in [3]. Also, Eq. (1) allows to see $\mathbf{x}(t)$ as the product of the magnitude $a(t)$, a *phasor* $\exp(\mathbf{j}\varphi(t))$ and a polarization vector $\mathbf{p}(t) \in L^2(\mathbb{C}^2)$. Interpretation of $\mathbf{p}(t)$ in terms of the classical polarization observables or quantum two-level systems (i.e. qubits) modelisation can be done through a 2nd

order description of $x(t)$. This is known as the *ray space* [6] description of $x(t)$.

III. RAY SPACE FOR BIVARIATE SIGNALS

The concept of ray space comes from quantum mechanics. It is defined as the set of equivalent classes for the equivalence relation $x \sim y \iff x = e^{i\alpha}y$, an equivalent class being called the state of the quantum system [6]. In terms of physical *observability*, this means that if $|\Psi(t)\rangle \in L^2(\mathbb{C}^2)$ is the state of a two-level quantum system, then for any $\lambda \in \mathbb{C}$ such that $|\lambda| = 1$ the states $\lambda|\Psi(t)\rangle$ and $|\Psi(t)\rangle$ are identical [6]. The ray space associated to $\lambda|\Psi(t)\rangle$ is totally described by $|\Psi(t)\rangle\langle\Psi(t)|$, the instantaneous covariance matrix of all $\lambda|\Psi(t)\rangle$. The analogy with bivariate signals is straightforward since for any real-valued function $\alpha(t)$ the two signals $x(t)$ and $e^{j\alpha(t)}x(t)$ have the same instantaneous covariance matrix $x(t)x^\dagger(t)$, where $(\cdot)^\dagger$ stands for the conjugate-transpose operation. After depicting the polarization inspired representation of the instantaneous covariance matrix, we give details on how it connects to a gauge invariant projective space for bivariate signals.

A. Instantaneous 2nd order representation

Second order characterization of a bivariate signal can be nicely formulated using the language of optics, as described in [3]. It actually refers to quadratic observables first introduced in optics by Stokes [7]. In particular, the *geometric* parameters $\theta(t)$ and $\chi(t)$ introduced in II-B through the polarization vector $\mathbf{p}(t)$ relate to the Poincaré sphere representation of $x(t)$ [7]. Given the expression of $x(t)$ in (1), the instantaneous covariance matrix $x(t)x^\dagger(t)$ can be expanded on the basis formed by the 2×2 Pauli matrices σ_i for $i = 0, 1, 2, 3$, with in particular $\sigma_0 = \mathbf{I}$ the identity matrix, in the following way:

$$x(t)x^\dagger(t) = \frac{1}{2} \left[S_0(t)\mathbf{I} + \sum_{i=1}^3 S_i(t)\sigma_i \right].$$

The coefficients of the expansion are known as the Stokes parameters. They relate to the parameters of bivariate AM-FM signal (1) in the following way:

$$\begin{aligned} S_0(t) &= a^2(t), \\ S_1(t) &= a^2(t) \cos 2\chi(t) \cos 2\theta(t), \\ S_2(t) &= a^2(t) \cos 2\chi(t) \sin 2\theta(t), \\ S_3(t) &= a^2(t) \sin 2\chi(t). \end{aligned}$$

The normalized version of the covariance matrix, denoted $\rho(t) \in \mathbb{C}^{2 \times 2}$ reads:

$$\rho(t) = \frac{x(t)x^\dagger(t)}{\|x(t)\|^2}$$

where $\|x(t)\|^2 = a^2(t) = S_0(t)$. The matrix $\rho(t)$ ¹ can thus be studied using its coordinates: $s_1(t) = S_1(t)/S_0(t)$, $s_2(t) = S_2(t)/S_0(t)$ and $s_3(t) = S_3(t)/S_0(t)$ known as the *normalized Stokes parameters* [7]. From their expression, it is obvious that $\rho(t)$ corresponds, at each instant t , to a point

¹In quantum mechanics, $\rho(t)$ is known as the *density matrix* [6].

on the sphere \mathcal{S}^2 of \mathbb{R}^3 with spherical angular coordinates $(2\theta(t), 2\chi(t))$. Fig. 1 illustrates the Poincaré sphere representation (also known as Bloch sphere in quantum optics) [7]. Parameters $(\theta(t), \chi(t))$ describe the instantaneous ellipse drawn by the bivariate AM-FM signal $x(t)$ given in (1). See also [3] for more details and examples.

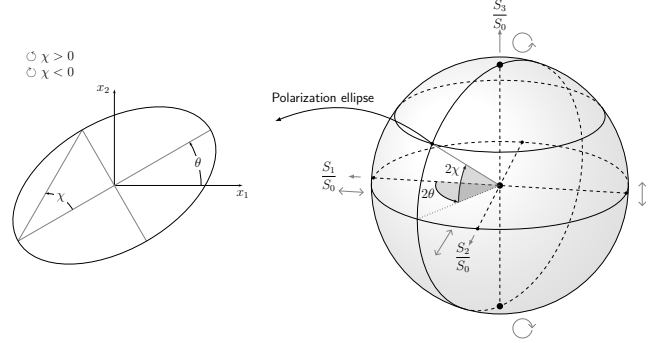


Fig. 1. Poincaré sphere representation and associated elliptical shape of the bivariate signal $x(t) = (x_1(t), x_2(t))^T$. One point on the sphere with coordinates $(S_1(t)/S_0(t); S_2(t)/S_0(t); S_3(t)/S_0(t))$ corresponds to one matrix $\rho(t)$.

For the bivariate signal $x(t)$, the instantaneous magnitude $a(t)$ and the instantaneous phase $\varphi(t)$ may change with time like for the univariate case. But in the bivariate case, $\theta(t)$ and $\chi(t)$ that describe the polarization state of the signal may also vary. This implies a time evolution of the normalized instantaneous covariance $\rho(t)$, and this may have unsuspected effects on $x(t)$ as described in Section IV. Before investigating the impact of changes in $\rho(t)$ on $x(t)$, we report some symmetry and invariance properties for $\rho(t)$.

B. Gauge invariance

As mentioned previously, several bivariate signals may have the same matrix $\rho(t)$. Consider a normalized bivariate signal, i.e. $\|x(t)\|^2 = 1$, then a transformation on $x(t)$ that leaves $\rho(t)$ unchanged is a so-called gauge invariant transformation. In our study, it takes the simple form:

$$\tilde{x}(t) = x(t)e^{j\alpha(t)}, \quad (2)$$

where $\alpha : \mathbb{R} \rightarrow \mathbb{R}$ is an arbitrary function, implying obviously that $x(t)x^\dagger(t) = \tilde{x}(t)\tilde{x}^\dagger(t) = \rho(t)$. As a consequence, $\rho(t)$ can be viewed as a point in the *projective space* $P(\mathbb{C})$ (in the bivariate case it is the Poincaré sphere), and to this point corresponds multiple possible values of $\tilde{x}(t)$. This fiber bundle structure is depicted in Fig. 2. The time evolution of $\rho(t)$ at the surface of the sphere can be thought as a smooth curve $\mathcal{C}(t)$ (see Fig. 2). To such a curve $\mathcal{C}(t)$ corresponds infinitely many different possible curves for $\tilde{x}(t)$ in the space of bivariate signals $L^2(\mathbb{C}^2)$.

The possible existence of an evolution (along a curve $\mathcal{C}(t)$) of $\rho(t)$ has direct consequences on the bivariate signal $x(t)$ itself. It may induce a non intuitive phase factor directly on $x(t)$: the *geometric phase*.

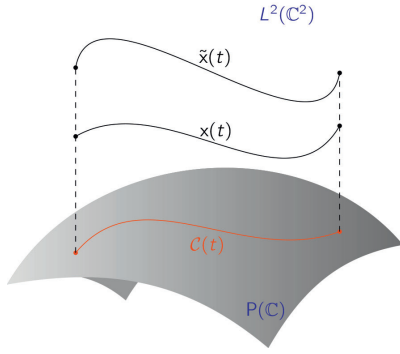


Fig. 2. Schematic representation of the $U(1)$ gauge invariance. A trajectory $\mathcal{C}(t)$ in the ray space $\mathcal{P}(\mathbb{C})$ of matrices $\rho(t)$ corresponds to an infinity of signals in the space $L^2(\mathbb{C}^2)$.

IV. GEOMETRIC PHASE

There exists several types of geometric phases which have been identified for classical or quantum systems [8]. The geometric phase we report here for bivariate signals belongs to the family of Berry-Pancharatnam phases [9], [10]. Its appearance is due to the evolution of $\rho(t)$ along the curve $\mathcal{C}(t)$. Its computation can be performed thanks to a class of invariants discovered in [11].

A. The $U(1)^{\times n}$ -invariant

As detailed in [6] and under some assumptions, an interesting family of invariant quantities can be constructed for bivariate signals. Remarkably, in the univariate case, these invariants vanish, a behaviour that relates to the fact that no geometric phase can exist for univariate signals. We briefly recall hereafter the construction of the invariant family that will then be used for the geometric phase evaluation in Section IV-C. Remember that we only consider *unitary* bivariate signals, i.e., such that $\|x(t)\|^2 = 1 \quad \forall t$. Now, given a set of n time instants (t_1, t_2, \dots, t_n) with $t_1 < t_2 < \dots < t_n$, the following complex-valued form:

$$\begin{aligned} & x^\dagger(t_1)x(t_2) \left[\prod_{i=2}^{n-1} x^\dagger(t_i)x(t_{i+1}) \right] x^\dagger(t_n)x(t_1) \\ &= x^\dagger(t_1) \left[\prod_{i=2}^n \rho(t_i) \right] x(t_1) \end{aligned} \quad (3)$$

is invariant to the gauge transformation given in (2), i.e. to the substitution, for any $i \in [1, n]$, of $x(t_i)$ by $e^{j\alpha(t_i)}x(t_i)$ for $\alpha(t_i) \in \mathbb{R}$. It is the circular product of the inner products between two successive vectors along the path designed by $x(t)$. Since the gauge transformation is a $U(1)$ transformation (multiplication by a unit complex number, i.e. a member of the $U(1)$ group), the quantity in (3) is a $U(1)^{\times n}$ -invariant quantity known as the Bargmann invariant [6]. This invariant will be used in Section IV-C to compute the geometric phase.

B. The geometric phase of bivariate signals

First, we briefly recall the reasoning detailed in [6]. Considering a unitary bivariate signal $x(t)$ and the gauge transformation $\tilde{x}(t) = e^{j\alpha(t)}x(t)$ for $t \in [t_1, t_n]$, we wish to define an invariant quantity that is concerned with the phase of $x(t)$.

The fact that $x^\dagger(t)x(t) = 1$ implies $\text{Re}(x^\dagger(t)\dot{x}(t)) = 0$, and thus:

$$x^\dagger(t)\dot{x}(t) = j \text{Im}(x^\dagger(t)\dot{x}(t))$$

where we used the notation $\frac{dx(t)}{dt} = \dot{x}(t)$. Applying the gauge transformation leads to

$$\tilde{x}^\dagger(t)\dot{\tilde{x}}(t) = j \text{Im}(\tilde{x}^\dagger(t)\dot{\tilde{x}}(t)) = j (\text{Im}(x^\dagger(t)\dot{x}(t)) + \dot{\alpha}(t))$$

As a consequence, given two instants $t_1 < t_2$, the quantity:

$$\begin{aligned} & \arg(\tilde{x}^\dagger(t_1)\tilde{x}(t_2)) - \text{Im} \int_{t_1}^{t_2} \tilde{x}^\dagger(t)\dot{\tilde{x}}(t) dt \\ &= \arg(x^\dagger(t_1)x(t_2)) - \text{Im} \int_{t_1}^{t_2} x^\dagger(t)\dot{x}(t) dt \end{aligned} \quad (4)$$

is proved to be gauge invariant. In addition, it can be shown [6] that it is also invariant to a reparametrization (i.e. changing t by a smooth monotonically increasing function of t). With this extra property, this invariant is called the *geometric phase* of the bivariate signal $x(t)$ during the time interval $t_2 - t_1$. Looking closely at (4), the two involved quantities correspond to two different “phases” between instants t_1 and t_2 : the *relative phase* $\Phi_{\text{rel}} = \arg(x^\dagger(t_1)x(t_2)) = \varphi(t_2) - \varphi(t_1)$ and the *dynamical phase* $\Phi_{\text{dyn}} = \text{Im} \int_{t_1}^{t_2} x^\dagger(t)\dot{x}(t) dt$. The *geometric phase* of a bivariate signal can be defined as follows.

Consider a unitary complex AM-FM bivariate signal $x(t)$ and its associated instantaneous covariance matrix $\rho(t)$. Given a smooth curve $\mathcal{C}(t)$ followed by $\rho(t)$ in the ray space, the geometric phase of $x(t)$ associated to $\mathcal{C}(t)$, and denoted $\Phi_{\text{geo}}[\mathcal{C}(t)]$, is given by:

$$\Phi_{\text{rel}}[\mathcal{C}(t)] - \Phi_{\text{dyn}}[\mathcal{C}(t)] = \pm \Phi_{\text{geo}}[\mathcal{C}(t)] \quad (5)$$

The sign of the geometric phase depends on the direction used to follow the path $\mathcal{C}(t)$. For the univariate case and as said previously, the geometric phase is null. It comes from the fact that relative and dynamical phases are equal for univariate signals, while it is no longer true in general for the bivariate case. There are however two particular cases for which the geometrical phase is null in the bivariate case. The first and obvious one occurs if the curve $\mathcal{C}(t)$ is restricted to a point on the sphere. In this case the polarisation parameters χ and θ are constant in time. The second and less intuitive one is the case of a geodesic curve (details and other properties can be found in [6] and [8]).

C. Computation of $\Phi_{\text{geo}}[\mathcal{C}(t)]$

In order to evaluate the geometric phase $\Phi_{\text{geo}}[\mathcal{C}(t)]$ of a bivariate signal, Eq. (5) can be implemented, requiring the computation of the relative and dynamical phases. However, another approach consists in using the Bargmann invariants introduced in IV-A, as proposed originally in [12]. Consider a unitary bivariate signal $x(t)$ and its associated instantaneous covariance matrix $\rho(t)$, together with a time interval Δt sampled at n time instants t_1, t_2, \dots, t_n with $\Delta t = t_n - t_1$. Assuming that $\rho(t)$ evolves along a path $\mathcal{C}(t)$ on the Poincaré sphere, the geometric phase acquired by $x(t)$ during Δt is given by:

$$\begin{aligned}\Phi_{\text{geo}}[\mathcal{C}(\Delta t)] &= -\arg(x^\dagger(t_1) [\prod_{i=2}^n \rho(t_i)] x(t_1)) \\ &= -\arg(\text{Tr}(\rho(t_1)\rho(t_2)\dots\rho(t_n)))\end{aligned}\quad (6)$$

which corresponds to the argument/phase of the Bargmann invariant introduced in (3). The geometric phase thus consists in the phase of the trace of the accumulated product of rank-1 instantaneous covariance matrices between the initial and final time instants $[t_1; t_n]$. It is worth noticing that the phase can only be non-null if more than two time instants are considered. This can be inferred from (6) due to the properties of the trace of a product of hermitian matrices (details in [12]). Note that in practice since (6) is only defined modulo 2π , estimating the geometric phase acquired during Δt requires to compute the phase for every t_1, t_2, \dots, t_n , before getting the correct geometric phase value for the duration Δt through phase unwrapping. The next section provides examples of this estimation on two bivariate signals.

V. EXAMPLES

In order to illustrate how the variations of the instantaneous covariance matrix of a bivariate signal can lead to the appearance of a geometric phase, we first consider a toy example where the time evolution of $\rho(t)$ follows a controlled path (geodesic triangle) on the Poincaré sphere. We then show how it can be used on a real bivariate signal from a seismic dataset.

A. Geodesic triangle on the Poincaré sphere

The original idea² of Pancharatnam was to consider the state of a totally polarized light beam undergoing a cyclic change of polarization [7]. He predicted that during such a change, a phase proportional to the area surrounded by the path in the polarization state space (Poincaré sphere) would be accumulated by the signal. Here, we consider the same idea with a bivariate narrow-band signal. We consider a pure frequency bivariate signal $x(t)$ (at 10 Hz) with real parts of components $x_1(t)$ and $x_2(t)$ displayed in Fig. 3.

The associated $\rho(t)$ matrix evolution is depicted in Fig. 4. The signal $x(t)$ starts in a purely linear polarization state at time t_0 with parameters $\theta(t_0) = -\pi/8$ and $\chi(t_0) = 0$. This corresponds to the blue point A in Fig. 4. As t grows from t_0 to t_1 , $\chi(t)$ remains constant while $\theta(t)$ grows linearly until it reaches $\pi/8$ (the great circle portion between points A and B on the equator). As shown in the lower panel of Fig. 3, no geometric phase is accumulated during this time evolution. Then, the signal evolves from t_1 to t_2 along the great circle connecting points B and C. At time t_2 , the polarization state is then $\theta(t_2) = +\pi/8$ and $\chi(t_2) = \pi/4$ (point C). During this interval, the polarization state moved from a linear state to a circular state (north pole at C). As depicted in the lower panel of Fig. 3, during this period of time, the geometric phase varies linearly and reaches a value of $-\pi/4$. Finally, the triangle ABC is closed with a transition from point C to A from time

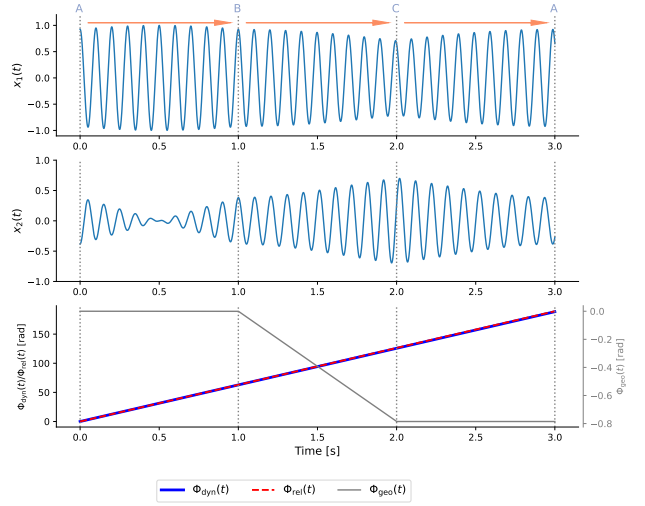


Fig. 3. Components $x_1(t)$ and $x_2(t)$ of the bivariate signal $x(t)$ which matrix $\rho(t)$ follows a geodesic triangle at the surface of the Poincaré sphere (see Fig. 4). Dotted grey lines indicate the time instants where corners of the geodesic triangle ABC are reached by $\rho(t)$. Lower panel shows the evolution of relative, dynamical and geometric phases.

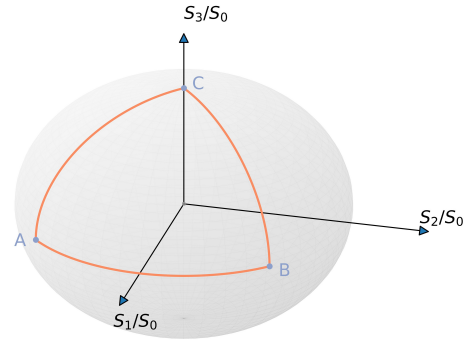


Fig. 4. Geodesic triangle trajectory followed by $\rho(t)$ on the Poincaré sphere for signal $x(t)$ displayed in Fig. 3. Point C is at the north pole while points A and B are on the equator.

t_2 to a time t_3 so that $\theta(t_3) = \theta(t_0)$ and $\chi(t_3) = \chi(t_0)$. No geometric phase is acquired along this path (see Fig. 3).

During the whole evolution of $\rho(t)$, a total geometric phase of $-\pi/4$ has been acquired by the bivariate signal. The minus sign would have been changed into a plus sign if the triangle had been travelled in the opposite direction. The value of the geometric phase corresponds to half the area encountered by the path, i.e. an eighth of the surface of the sphere. The phase shift on the bivariate signal $x(t)$ can be seen in Fig. 3 where the signal at time $t_0 = 0s$ (start at A) and time $t_3 = 3s$ (arrival back at A) is phase shifted by $\Phi_{\text{geo}}[\mathcal{C}(t)]$, $\mathcal{C}(t)$ being the geodesic triangle ABC depicted in orange in Fig. 4.

B. Seismic signal from the Gresivaudan valley

We consider a seismic signal recorded in 1997 by the first author and colleagues near Grenoble in the Gresivaudan valley. The original dataset consists in the recording of 47 two-

²It was actually a *Gedankenexperiment* at the time he proposed it.

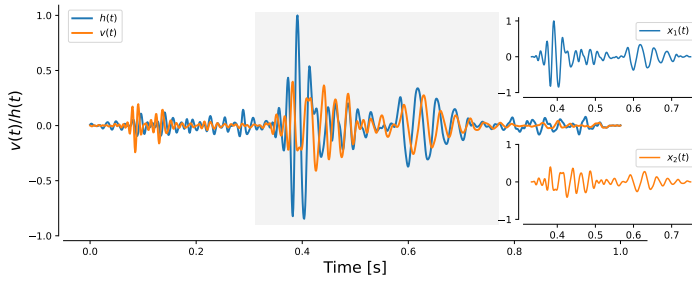


Fig. 5. Original vertical $v(t)$ and horizontal $h(t)$ components and seismic signal. The selected time interval is displayed with grey background. Associated $x_1(t)$ and $x_2(t)$ of the bivariate signal $x(t)$ to be used for geometric phase estimation are given in upper and lower insets.

components seismometers, placed in a linear array shape, that recorded the vibrations of the ground after an impulsive source was created nearby the array (hammer shock on an iron bar). Each seismometer records two signals: one horizontal $h(t)$ and one vertical $v(t)$. The signals considered were recorded by sensor No. 42 placed approximately 50 meters from the source. The corresponding $h(t)$ and $v(t)$ signals are shown in Fig. 5, where two Rayleigh waves impinge the sensor between 0.3s and 0.8s (grey area). Our analysis is performed on this time interval. The corresponding components $x_1(t)$ and $x_2(t)$ of the signal $x(t)$ considered are displayed in the two insets of Fig. 5. To perform the geometric phase estimation and analysis, the signal $x(t)$ was band-pass filtered around 8 Hz. This allows us to validate the narrow-band AM-FM hypothesis for the geometric phase existence and interpretation. The resulting components of $x(t)$ and phases (relative, dynamical and geometric) are given in Fig. 6. Several regimes for Φ_{geo} during the time interval considered appear. During the time period where the Rayleigh modes hit the sensor, the geometric phase does not increase (time intervals 0.35s – 0.45s and 0.6s – 0.7s) which means that the polarization state is constant during these periods. In between those intervals, the geometric phase increases or decreases depending on the polarization variations in the bivariate signal. The variations in the sign of the geometric phase are also interesting. The geometric phase can accumulate positive or negative values along time. This actually depends on the evolution of $\rho(t)$ on the Poincaré sphere, i.e. the direction (direct or reverse) with which it surrounds an area. From Fig. 7, one can see that many changes occur during the time interval considered due to the complicated path followed. Obviously, there is also an effect of the ambient noise on the path smoothness, impacting geometric phase estimation. The study of such effects is left for further work.

This example demonstrates the potential use of the geometric phase for real bivariate signal analysis and its possible use to highlight distinctive features related to instantaneous covariance variations.

REFERENCES

- [1] P. Flandrin. *Time-frequency/Time-scale analysis*. Academic Press, San Diego, 1999.
- [2] J.M. Lilly, and S. C. Olhede, "Bivariate instantaneous frequency and bandwidth", *IEEE Trans. on Signal Processing*, vol. 58, no. 2, 2010.

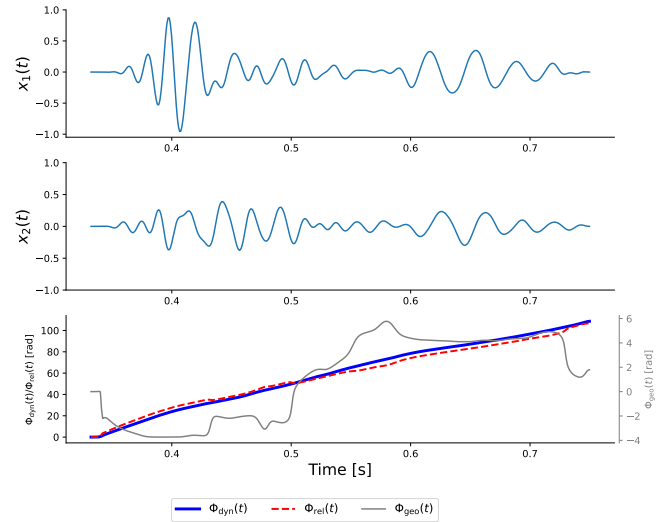


Fig. 6. Components $x_1(t)$ and $x_2(t)$ of the bivariate seismic signal $x(t)$. The geometric phase (equal to the difference between relative and dynamical phases) accumulated during the time interval in displayed grey.

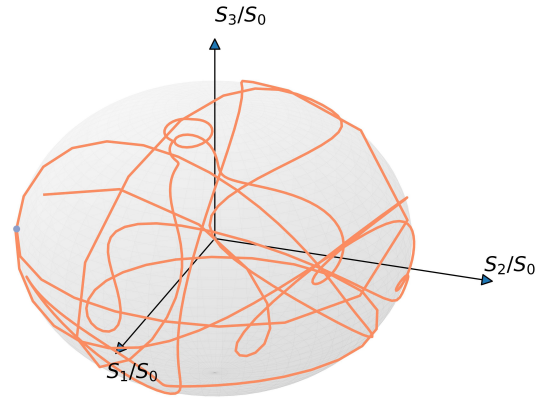


Fig. 7. Trajectory followed by $\rho(t)$ for seismic signal $x(t)$ depicted in Fig. 6. The complexity of the trajectory reveals the numerous variations of $\rho(t)$.

- [3] J. Flamant, N. Le Bihan, and P. Chainais, "Time-frequency analysis of bivariate signals", *Applied and Computational Harmonic Analysis*, vol. 46, no. 2, 2019.
- [4] B. Picinbono, "On instantaneous amplitude and phase of signals", *IEEE Trans. on Signal Processing*, vol. 45, No. 3, 1997.
- [5] J. Gonella, "A rotary-component method for analysing meteorological and oceanographic vector time series", *Deep Sea Research And Oceanographic Abstracts*, 19, 1972.
- [6] N. Mukunda and R. Simon, "Quantum kinematic approach to the geometric phase I. General formalism", *Annals of Physics*, 228, 1993.
- [7] C. Brosseau. *Fundamentals of polarized light: a statistical optics approach*. Wiley, 1998.
- [8] A. Shapere, and F. Wilczek, "Geometric phases in physics", World Scientific, 1989.
- [9] S. Pancharatnam, "Generalized theory of interference, and its applications", *Proc. of Indian Acad. Sci.*, Vol. 44, 1956.
- [10] M.V. Berry, "The adiabatic phase and Pancharatnam's phase for polarized light", *Journal of Modern Optics*, Vol. 34, No. 11, 1987.
- [11] V. Bargmann, "Note on Wigner's theorem on symmetry operations", *Journal of Mathematical Physics*, vol. 5, No. 7, 1964.
- [12] E.M. Rabei, Arvind, N. Mukunda, and R. Simon, "Bargmann invariants and geometric phases: a generalized connection", *Phys. Rev. A*, Vol. 60, No. 5, 1999.